

Measurement of collective dynamics in small and large systems with the ATLAS detector

Somadutta Bhatta (On behalf of the ATLAS Collaboration)^{a,*}

^a*Stony Brook University,*

Stony Brook, New York, USA-11790

E-mail: somadutta.bhatta@stonybrook.edu

Investigating collectivity in proton-proton (pp) and proton-nucleus ($p + A$) collisions is essential for understanding the mechanism of formation of Quark Gluon Plasma (QGP). In pp collisions at $\sqrt{s_{NN}} = 13$ TeV, ATLAS has reported no impact on flow coefficients when excluding low- p_T jets, indicating collectivity in small systems does not originate from hard processes. Comparing flow decorrelation in Xe+Xe and pp collisions at $\sqrt{s_{NN}} = 5.44$ TeV and 5 TeV respectively, underscores the role of sub-nucleonic fluctuations in determining longitudinal energy deposition. ATLAS has also reported a significant correlation between event-wise flow and transverse momentum fluctuations in Xe+Xe and Pb+Pb collisions at $\sqrt{s_{NN}} = 5.44$ TeV and 5 TeV respectively, emphasizing the role of nuclear structure in accurately describing bulk observables in heavy-ion collisions and provides the first experimental evidence from a high-energy experiment for a significant triaxiality in ^{129}Xe .

*The European Physical Society Conference on High Energy Physics (EPS-HEP2023)
21-25 August 2023
Hamburg, Germany*

*Speaker

1. Introduction and Measurements

Heavy-ion collisions at the Large Hadron Collider produce QGP, whose space-time evolution is well described by relativistic viscous hydrodynamics. Driven by the large pressure gradients, the QGP expands rapidly in the transverse plane and converts the spatial anisotropy in the initial state into momentum anisotropy in the final state. The collective expansion in each event is quantified by a Fourier expansion of particle distribution in azimuth given by $\frac{dN}{d\phi} = \frac{N}{2\pi} (1 + 2 \sum_{n=1}^{\infty} v_n \cos n(\phi - \Phi_n))$, where v_n and Φ_n represent the amplitude and phase of the n^{th} -order azimuthal flow vector $V_n = v_n e^{in\Phi_n}$. Collectivity in this context means that the produced particles exhibit a common property, such as a common velocity field or a common direction [1]. Model calculations show that the V_n is approximately proportional to initial state eccentricity \mathcal{E}_n for $n = 2$ and 3 , as well as for $n = 4$ in central collisions [2]. In addition, the fluctuations in the size of the overlap area in the initial state give rise to fluctuations in radial flow, which, in turn, lead to event-by-event fluctuation of the average transverse momentum ($\langle p_T \rangle$).

The most intriguing feature of the azimuthal anisotropies is the “ridge” behavior, which is an enhancement in the production of particles with small azimuthal angle (ϕ) separation extending over a large range of pseudorapidity (η) separation [3]. The presence of the ridge in heavy-ion collisions is typically attributed to hydrodynamic flow and is viewed as a signature of collective behavior and the formation of QGP. In smaller collision systems such as $p+A$ or pp , the presence of the ridge challenges the notion that collective behavior is exclusive to QGP formation and has led to several phenomenological models attributing the origin of long-range behavior to hard or semi-hard processes. In these processes, multi-particle correlations between outgoing partons may arise due to saturation of the parton configurations in the incident hadrons [4]. If the long-range correlations arise due to hard or semi-hard processes, removing particles associated with jets from the analysis would weaken the long-range correlation.

To investigate the influence of hard processes on the origin of collectivity in small systems, ATLAS has probed the role of semi-hard and hard processes on collective behavior observed in small systems [5]. The events were systematically categorized into five distinct groups based on their two-particle correlations, each representing varying contributions from particles produced by jets, all falling within a p_T -range of 4 GeV. These five categories are: $h-h$, which denotes the analysis of all particles; $h^{\text{UE}} - h^{\text{J}}$, indicating correlations between one particle originating from a jet and another from the underlying event; and three classes pertaining to 2-Particle Correlations between particles from the underlying event: **AllEvents**, where the analysis includes tracks within one unit in η from any jet above the chosen threshold of 10 GeV, which are excluded from the 2-Particle Correlation analysis; **NoJet**, where the analysis is carried out on events that do not possess a single jet with transverse momentum (p_T) greater than the chosen threshold, thereby encompassing events primarily governed by soft processes; and **WithJet**, representing the analysis performed on events featuring at least one jet with p_T greater than the chosen p_T threshold.

Figure 1 compares measured v_2 with varying contributions from jets. It is evident that both integrated v_2 and differential $v_2(p_T)$ remain unaltered by the presence or absence of jets. Consequently, this measurement led to the conclusion that hard scatterings do not play a role in generating long-range correlations, effectively ruling out their contribution to the ridge phenomenon.

To explore the impact of sub-nucleonic fluctuations on collectivity, ATLAS has measured

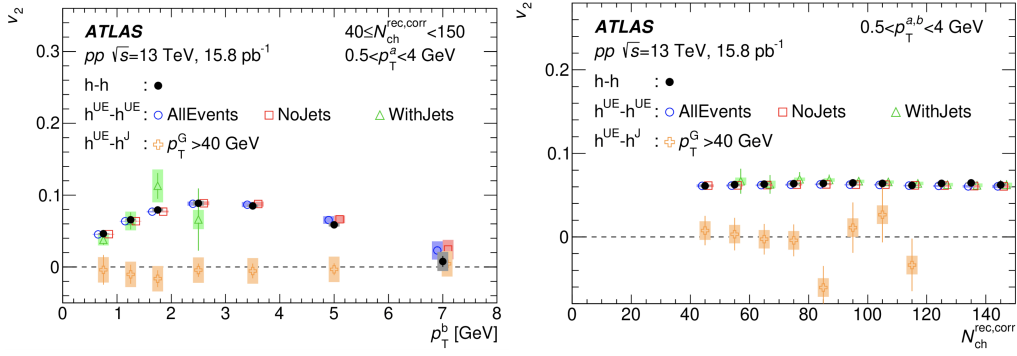


Figure 1: (Left) p_T dependence of the v_2 obtained for the 40–150 multiplicity interval. (Right) v_2 as a function of the (efficiency corrected) multiplicity. The data-points for the Inclusive sample are drawn at the nominal values, AllEvents and NoJet points are shifted slightly for clarity. Data-points for the WithJet sample are evaluated over coarser multiplicity intervals to reduce statistical uncertainties. The error bars and shaded bands correspond to statistical and systematic uncertainties, respectively [5].

decorrelation in smaller systems. Decorrelation refers to the reduction in the strength of flow-correlation with increasing η gaps between correlated particles. In this context, peripheral Xe+Xe and pp collisions provide simplified scenarios for understanding the longitudinal structure of QGP [6]. Decorrelation arises from the fact that in heavy ion collisions, owing to initial state fluctuations, deposited energy and the transverse shape of the fireball is not boost invariant. Model studies have shown that preferential emission by forward and backward-moving participant nucleons produce particles preferably in the forward direction, leading to an event-by-event torqued fireball. This leads to an asymmetry of flow magnitude as well as a “Twist” of the symmetry plane in the longitudinal direction on an event-by-event basis [7, 8]. Previous measurements conducted by the ATLAS collaboration had revealed that state-of-the-art hydrodynamic models are inadequate in describing the longitudinal structure of initial energy deposition[9].

Figure 2 shows the comparison of the decorrelation signal (F_2) for pp and Xe+Xe collisions [6]. At the lowest multiplicities, the decorrelations observed in pp collisions are close to those in Xe+Xe collisions, implying that Xe+Xe events with low multiplicities are predominantly characterized by single nucleon-nucleon configurations. Conversely, as multiplicities increase, the observed F_2 values in Xe+Xe collisions diminish, signifying a distinct mechanism for additional particle production in these two systems. As a result, this study concludes that the correlation between the geometry of the initial state and overall particle production exhibits variations at sub-nucleonic scales compared to nucleonic scales. Furthermore, the predictions from the AMPT model, which involves two-color strings spanning a significant longitudinal extent in pp collisions, do not align well with the data. This suggests a need for further refinement and fine-tuning of longitudinal modeling to describe the data accurately.

In addition to generating anisotropic flow, the collective response to the overall transverse size (R) in the initial state also leads to a large “radial flow”, reflected by an increase of the $[p_T]$. Any correlated fluctuations between the \mathcal{E}_n and R in the initial state are expected to generate a dynamical correlation between v_n and $[p_T]$ in the final state. A three-particle correlator has been proposed to

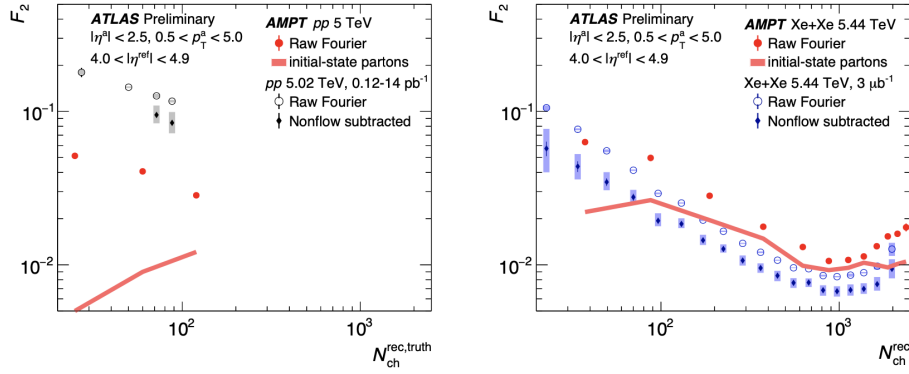


Figure 2: A comparison of AMPT theory calculations to the 5 TeV pp (left) and 5.44 TeV Xe+Xe (right) results. In data, the raw F_2 values are shown as a function of N_{rec} . Additionally, the subtracted F_2 values are shown. The statistical uncertainties are drawn as vertical lines. The systematic uncertainties are plotted as bands [6].

quantify this correlation [10]:

$$\rho_n = \frac{\langle\langle v_n^2 \delta p_T \rangle\rangle}{\sqrt{\left(\langle v_n^4 \rangle - \langle v_n^2 \rangle^2\right)} \sqrt{\langle\langle \delta p_T \delta p_T \rangle\rangle}}, \quad (1)$$

where the averages are over events with similar particle multiplicity.

An investigation on the system-size dependence of $v_n - [p_T]$ correlation is performed in $^{129}\text{Xe} + ^{129}\text{Xe}$ collisions and comparing them with $^{208}\text{Pb} + ^{208}\text{Pb}$ collisions at ATLAS [11]. Recent measurements show that the ρ_n exhibits significant differences between these two systems, especially in the central collisions due to the deformation of nuclear structure in ^{129}Xe . Deformations in nuclear structure is generally parametrized using $R(\theta, \phi) = R_0 (1 + \beta[\cos \gamma Y_{2,0} + \sin \gamma Y_{2,2}])$ where R_0 is the nuclear radius, $Y_{l,m}$ are spherical harmonics, β , and γ are quadrupole deformation parameters. β is the magnitude of overall deformation, while $\gamma (0 \leq \gamma \leq 60^\circ)$ describes the length imbalance between the three axes of the spheroid, called ‘‘Triaxiality’’. Recent models indicate $\rho_2 \approx a + b \cos(3\gamma)\beta^3$ [12], where, a and b are values for spherical nuclei. In addition to these initial-state-driven long-range global correlations, the $v_n - [p_T]$ correlation measurement may have short-range ‘‘non-flow’’ correlations from resonance decays and jets. The non-flow correlation is suppressed by requiring correlation between particles from different subevents separated in η [13]. In peripheral centralities, a double sign change in ρ_2 is predicted as evidence of the existence of initial momentum anisotropy [14].

Figure 3 displays ρ_2 for Pb+Pb collisions versus $N_{\text{ch}}^{\text{rec}}$ compared with different models incorporating initial and final state dynamics. In the 0–10% centrality interval, where the effects of nuclear deformation are important, all models generally show reasonable agreement with each other and with the data. In particular, the Trajectum model quantitatively reproduces the ordering between $0.5 < p_T < 2$ GeV and $0.5 < p_T < 5$ GeV. In the peripheral collisions, all model predictions for ρ_2 show a sharp decrease and a sign-change, qualitatively consistent with the ATLAS data.

Figure 3 also compares ρ_2 (0–20% centrality) with Trento model to constrain γ_{Xe} [15]. Due to large quadrupole deformation in ^{129}Xe ($\beta_{\text{Xe}} \sim 0.2$), ρ_2 is sensitive to γ_{Xe} . The Trento model

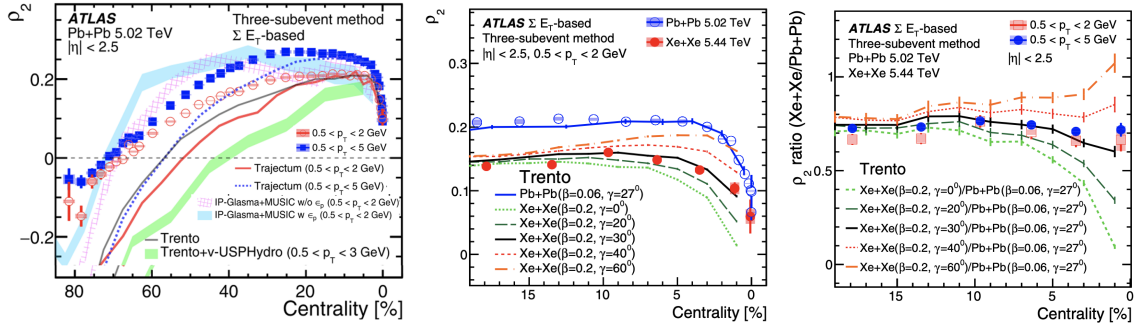


Figure 3: (Left) ρ_2 values in Pb+Pb collisions in two p_T -ranges and $|\eta| < 2.5$ compared with various models: Trento and Trajectum models in solid lines and v-USPhydro and IP-Glasma+MUSIC hydrodynamic models in shaded bands, which represent the statistical uncertainties of the model calculations. (Center) Comparison of ρ_2 in Xe+Xe and Pb+Pb collisions with the Trento model for various quadrupole deformation parameter values in $0.5 < p_T < 2$ GeV as a function of centrality. (Right) Comparison of ρ_2 ratios, $\rho_{2,\text{Xe+Xe}}/\rho_{2,\text{Pb+Pb}}$, with the Trento model for various quadrupole deformation parameter values in two p_T -ranges. The Trento model results are connected by lines for better visualization [11].

predictions agree with the ρ_2 measured for $0.5 < p_T < 2$ GeV for both Pb+Pb and Xe+Xe collisions for appropriate values of deformation parameters. To nullify p_T dependence, ratios of ρ_2 between Xe+Xe and Pb+Pb are computed for two p_T -ranges and compared in Figure 3. In 10–20% centrality, where triaxiality has a minor impact, the model and data ratio closely match. In 0–10% centrality, where ρ_2 strongly depends on triaxiality, the comparison favors $\gamma_{\text{Xe}} \sim 30^\circ$. Thus, ATLAS provided the first experimental evidence from the high-energy collision of a significant triaxiality in ^{129}Xe using ρ_2 . A recent model study underscores the accuracy of extracting γ only when nuclear fluctuations in γ are small [16]. Consequently, the $\rho_{(2,\text{Xe})}/\rho_{(2,\text{Pb})}$ ratio supports the triaxial shape of ^{129}Xe , but only under the condition that the fluctuations in γ_{Xe} are not extensive.

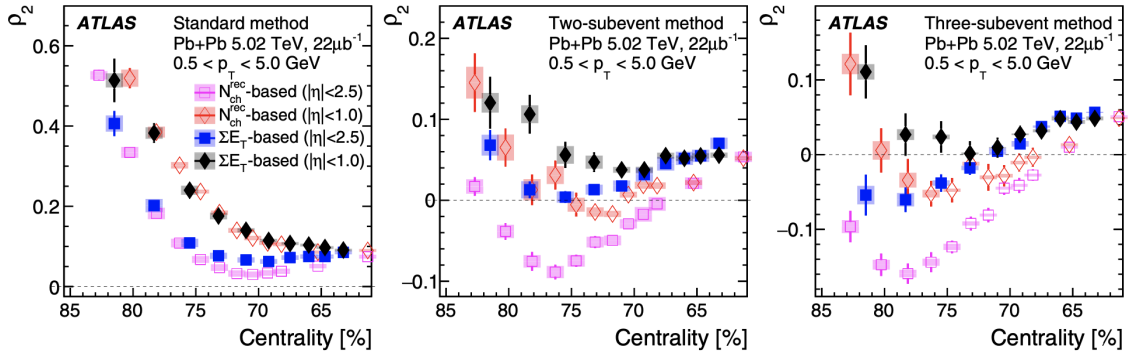


Figure 4: The centrality dependence of ρ_2 in Pb+Pb collisions in the peripheral region of 60–84% for the standard method (left), two-subevent method (middle) and three-subevent method (right), compared between the $N_{\text{ch}}^{\text{rec}}$ -based and ΣE_T -based event-averaging procedures and two η -ranges. The error bars and shaded boxes represent statistical and systematic uncertainties, respectively [11].

Figure 4 illustrates ρ_2 values in Pb+Pb collisions for particles originating from various η regions and employing different subevent methods. Additionally, it demonstrates measurements

as a function of particle production in central versus forward rapidities, denoted as $N_{\text{ch}}^{\text{rec}}$ and ΣE_{T} respectively. While some hints of a double sign change in ρ_2 in peripheral centralities are observed, it is inconclusive due to the limited range of centrality under study. The extent of the sign change depends on factors like centrality determination methods based on $N_{\text{ch}}^{\text{rec}}$ or ΣE_{T} and the presence of short-range correlations like jets. Future measurements in smaller systems may help isolate these effects and support the search for evidence of initial momentum anisotropy in heavy-ion collisions.

2. Summary

In summary, ATLAS has demonstrated using pp collisions at $\sqrt{s_{\text{NN}}} = 13$ TeV, that hard scatterings do not contribute to long-range correlations, ruling out their role in ridge behavior. Decorrelation measurements in pp collisions at $\sqrt{s_{\text{NN}}} = 5$ TeV and Xe+Xe collisions at $\sqrt{s_{\text{NN}}} = 5.44$ TeV show that the correlation between the initial-state geometry and overall particle production differs at sub-nucleonic scales compared to nucleonic scales. Through examinations of Pb+Pb collisions at $\sqrt{s_{\text{NN}}} = 5$ TeV and Xe+Xe collisions at $\sqrt{s_{\text{NN}}} = 5.44$ TeV, ATLAS has provided the first experimental evidence from the high-energy collision of a significant triaxiality in ^{129}Xe using ρ_2 and constraints $\gamma_{\text{Xe}} \sim 30^\circ$. In addition, the ρ_2 also shows a hint of double sign change behavior in peripheral centralities similar to those expected from the existence of initial state momentum anisotropy. Further investigation in smaller systems is necessary for more conclusive evidence owing to the existence of additional effects like centrality fluctuations and non-flow. These comprehensive findings provide crucial contributions to constrain the modeling of heavy-ion collisions and to understand the origin of collective behavior in the QGP medium.

References

- [1] N. Herrmann, J. P. Wessels, and T. Wienold. “Collective flow in heavy ion collisions”. *Ann. Rev. Nucl. Part. Sci.* 49 (1999), pp. 581–632. DOI: [10.1146/annurev.nucl.49.1.581](https://doi.org/10.1146/annurev.nucl.49.1.581).
- [2] Derek Teaney and Li Yan. “Triangularity and Dipole Asymmetry in Heavy Ion Collisions”. *Phys. Rev. C* 83 (2011), p. 064904. DOI: [10.1103/PhysRevC.83.064904](https://doi.org/10.1103/PhysRevC.83.064904). arXiv: [1010.1876 \[nucl-th\]](https://arxiv.org/abs/1010.1876).
- [3] ATLAS Collaboration. “Measurements of long-range azimuthal anisotropies and associated Fourier coefficients for pp collisions at $\sqrt{s} = 5.02$ and 13 TeV and $p+\text{Pb}$ collisions at $\sqrt{s_{\text{NN}}} = 5.02$ TeV with the ATLAS detector”. *Phys. Rev. C* 96.2 (2017), p. 024908. DOI: [10.1103/PhysRevC.96.024908](https://doi.org/10.1103/PhysRevC.96.024908). arXiv: [1609.06213 \[nucl-ex\]](https://arxiv.org/abs/1609.06213).
- [4] Adrian Dumitru et al. “The Ridge in proton-proton collisions at the LHC”. *Phys. Lett. B* 697 (2011), pp. 21–25. DOI: [10.1016/j.physletb.2011.01.024](https://doi.org/10.1016/j.physletb.2011.01.024). arXiv: [1009.5295 \[hep-ph\]](https://arxiv.org/abs/1009.5295).
- [5] ATLAS Collaboration. “Measurement of the sensitivity of two particle correlations in pp collisions at $\sqrt{s} = 13$ TeV to the presence of jets with the ATLAS detector” (June 2020).
- [6] ATLAS Collaboration. “Measurements of longitudinal flow decorrelations in pp and Xe+Xe collisions with the ATLAS detector” (Aug. 2023). arXiv: [2308.16745 \[nucl-ex\]](https://arxiv.org/abs/2308.16745).

- [7] Piotr Bozek, Wojciech Broniowski, and Joao Moreira. “Torqued fireballs in relativistic heavy-ion collisions”. *Phys. Rev. C* 83 (2011), p. 034911. DOI: [10.1103/PhysRevC.83.034911](https://doi.org/10.1103/PhysRevC.83.034911). arXiv: [1011.3354](https://arxiv.org/abs/1011.3354) [nucl-th].
- [8] Jianguong Jia and Peng Huo. “Forward-backward eccentricity and participant-plane angle fluctuations and their influences on longitudinal dynamics of collective flow”. *Phys. Rev. C* 90.3 (2014), p. 034915. DOI: [10.1103/PhysRevC.90.034915](https://doi.org/10.1103/PhysRevC.90.034915). arXiv: [1403.6077](https://arxiv.org/abs/1403.6077) [nucl-th].
- [9] ATLAS Collaboration. “Longitudinal Flow Decorrelations in Xe+Xe Collisions at $\sqrt{s_{NN}} = 5.44$ TeV with the ATLAS Detector”. *Phys. Rev. Lett.* 126.12 (2021), p. 122301. DOI: [10.1103/PhysRevLett.126.122301](https://doi.org/10.1103/PhysRevLett.126.122301). arXiv: [2001.04201](https://arxiv.org/abs/2001.04201) [nucl-ex].
- [10] Piotr Bozek. “Transverse-momentum–flow correlations in relativistic heavy-ion collisions”. *Phys. Rev. C* 93.4 (2016), p. 044908. DOI: [10.1103/PhysRevC.93.044908](https://doi.org/10.1103/PhysRevC.93.044908). arXiv: [1601.04513](https://arxiv.org/abs/1601.04513) [nucl-th].
- [11] ATLAS Collaboration. “Correlations between flow and transverse momentum in Xe+Xe and Pb+Pb collisions at the LHC with the ATLAS detector: A probe of the heavy-ion initial state and nuclear deformation”. *Phys. Rev. C* 107.5 (2023), p. 054910. DOI: [10.1103/PhysRevC.107.054910](https://doi.org/10.1103/PhysRevC.107.054910). arXiv: [2205.00039](https://arxiv.org/abs/2205.00039) [nucl-ex].
- [12] Jianguong Jia. “Probing triaxial deformation of atomic nuclei in high-energy heavy ion collisions”. *Phys. Rev. C* 105.4 (2022), p. 044905. DOI: [10.1103/PhysRevC.105.044905](https://doi.org/10.1103/PhysRevC.105.044905). arXiv: [2109.00604](https://arxiv.org/abs/2109.00604) [nucl-th].
- [13] Jianguong Jia, Mingliang Zhou, and Adam Trzupek. “Revealing long-range multiparticle collectivity in small collision systems via subevent cumulants”. *Phys. Rev. C* 96.3 (2017), p. 034906. DOI: [10.1103/PhysRevC.96.034906](https://doi.org/10.1103/PhysRevC.96.034906). arXiv: [1701.03830](https://arxiv.org/abs/1701.03830) [nucl-th].
- [14] Giuliano Giacalone, Björn Schenke, and Chun Shen. “Observable signatures of initial state momentum anisotropies in nuclear collisions”. *Phys. Rev. Lett.* 125.19 (2020), p. 192301. DOI: [10.1103/PhysRevLett.125.192301](https://doi.org/10.1103/PhysRevLett.125.192301). arXiv: [2006.15721](https://arxiv.org/abs/2006.15721) [nucl-th].
- [15] Benjamin Bally et al. “Evidence of the triaxial structure of ^{129}Xe at the Large Hadron Collider”. *Phys. Rev. Lett.* 128.8 (2022), p. 082301. DOI: [10.1103/PhysRevLett.128.082301](https://doi.org/10.1103/PhysRevLett.128.082301). arXiv: [2108.09578](https://arxiv.org/abs/2108.09578) [nucl-th].
- [16] Aman Dimri, Somadutta Bhatta, and Jianguong Jia. “Impact of nuclear shape fluctuations in high-energy heavy ion collisions”. *Eur. Phys. J. A* 59.3 (2023), p. 45. DOI: [10.1140/epja/s10050-023-00965-1](https://doi.org/10.1140/epja/s10050-023-00965-1). arXiv: [2301.03556](https://arxiv.org/abs/2301.03556) [nucl-th].